



A Mass Spectrometry-Based Profiling of Interactomes of Viral DDB1- and Cullin Ubiquitin Ligase-Binding Proteins Reveals NF- κ B Inhibitory Activity of the HIV-2-Encoded Vpx

OPEN ACCESS

Edited by:

Uday Kishore,
Brunel University London,
United Kingdom

Reviewed by:

Even Fossum,
Oslo University Hospital, Norway
Xiaocui He,
La Jolla Institute for Allergy and
Immunology (LJI), United States

*Correspondence:

Mirko Trilling
mirko.trilling@uni-due.de

† Present Address:

Jassin Rashidi-Alavijeh,
Department of Gastroenterology and
Hepatology, University Hospital Essen,
University of Duisburg-Essen, Essen,
Germany

Specialty section:

This article was submitted to
Molecular Innate Immunity,
a section of the journal
Frontiers in Immunology

Received: 03 September 2018

Accepted: 04 December 2018

Published: 19 December 2018

Citation:

Landsberg CD, Megger DA, Hotter D, Rückborn MU, Eilbrecht M, Rashidi-Alavijeh J, Howe S, Heinrichs S, Sauter D, Sitek B, Le-Trilling VTK and Trilling M (2018) A Mass Spectrometry-Based Profiling of Interactomes of Viral DDB1- and Cullin Ubiquitin Ligase-Binding Proteins Reveals NF- κ B Inhibitory Activity of the HIV-2-Encoded Vpx. *Front. Immunol.* 9:2978. doi: 10.3389/fimmu.2018.02978

Christine D. Landsberg¹, Dominik A. Megger^{1,2}, Dominik Hotter³, Meike U. Rückborn¹, Mareike Eilbrecht¹, Jassin Rashidi-Alavijeh[†], Sebastian Howe¹, Stefan Heinrichs⁴, Daniel Sauter³, Barbara Sitek², Vu Thuy Khanh Le-Trilling¹ and Mirko Trilling^{1*}

¹ Institute for Virology, University Hospital Essen, University of Duisburg-Essen, Essen, Germany, ² Medical Proteome-Center, Ruhr-University Bochum, Bochum, Germany, ³ Institute of Molecular Virology, Ulm University Medical Center, Ulm, Germany,

⁴ Institute for Transfusion Medicine, University Hospital Essen, University of Duisburg-Essen, Essen, Germany

Viruses and hosts are situated in a molecular arms race. To avoid morbidity and mortality, hosts evolved antiviral restriction factors. These restriction factors exert selection pressure on the viruses and drive viral evolution toward increasingly efficient immune antagonists. Numerous viruses exploit cellular DNA damage-binding protein 1 (DDB1)-containing Cullin RocA ubiquitin ligases (CRLs) to induce the ubiquitination and subsequent proteasomal degradation of antiviral factors expressed by their hosts. To establish a comprehensive understanding of the underlying protein interaction networks, we performed immuno-affinity precipitations for a panel of DDB1-interacting proteins derived from viruses such as mouse cytomegalovirus (MCMV, Murid herpesvirus [MuHV] 1), rat cytomegalovirus Maastricht MuHV2, rat cytomegalovirus English MuHV8, human cytomegalovirus (HCMV), hepatitis B virus (HBV), and human immunodeficiency virus (HIV). Cellular interaction partners were identified and quantified by mass spectrometry (MS) and validated by classical biochemistry. The comparative approach enabled us to separate unspecific interactions from specific binding partners and revealed remarkable differences in the strength of interaction with DDB1. Our analysis confirmed several previously described interactions like the interaction of the MCMV-encoded interferon antagonist pM27 with STAT2. We extended known interactions to paralogous proteins like the interaction of the HBV-encoded HBx with different Spindlin proteins and documented interactions for the first time, which explain functional data like the interaction of the HIV-2-encoded Vpr with Bax. Additionally, several novel interactions were identified, such as the association of the HIV-2-encoded Vpx with the transcription factor RelA (also called p65). For the latter interaction, we documented a functional relevance in antagonizing NF- κ B-driven gene expression. The mutation of the DDB1 binding interface of Vpx significantly impaired

NF- κ B inhibition, indicating that Vpx counteracts NF- κ B signaling by a DDB1- and CRL-dependent mechanism. In summary, our findings improve the understanding of how viral pathogens hijack cellular DDB1 and CRLs to ensure efficient replication despite the expression of host restriction factors.

Keywords: interaction partner, mass spectrometry (MS), human immunodeficiency virus (HIV), hepatitis B virus (HBV), cytomegalovirus, NF- κ B, interferon, DNA damage-binding protein (DDB1)

INTRODUCTION

In response to viral infections, host cells have evolved a plethora of so-called restriction factors that inhibit specific steps of the viral replication cycle, thereby limiting the damage caused by infections. Several of these restriction factors are encoded by interferon (IFN)-stimulated genes (ISG) (1, 2). The antiviral activity elicited by restriction factors in turn exerts strong selection pressure on viruses, which have evolved sophisticated evasion and counteraction strategies (3).

One irreversible mechanism by which viral accessory proteins counteract restriction factors is the induction of their proteolytic degradation. To achieve this, viruses frequently exploit cellular pathways of protein degradation such as the proteasome. Although several pathways may target proteins for proteasomal degradation, ubiquitination is considered the most important one (4). Ubiquitin (Ub) is a small protein that is covalently linked to proteins acting as a molecular tag to mediate the recognition by the proteasome (5). Viruses inducing the proteasomal degradation of host restriction factors via ubiquitination (6, 7) often lose their replication capacity, if the Ub conjugation machinery or the proteasome is inactivated (8–12). However, an inhibition of the proteasome alters the abundance of more than 80% of all cellular proteins (13). Not surprisingly, such regimes are associated with severe toxicity limiting their application as antiviral drugs—despite their FDA approval as tumor drugs (e.g., Bortezomib). A specific inhibition of individual Ub ligases might limit side effects to levels tolerable in the context of antiviral therapies.

Cytomegaloviruses inhibit IFN-induced Jak-STAT signaling (14–20). Cytomegaloviruses exploit DNA damage-binding protein 1 (DDB1) and Cullin RocA ubiquitin ligases (CRLs) to antagonize IFN signaling (16, 21). In uninfected cells, DDB1 fulfills several cellular functions including nucleotide excision DNA repair (22). Consistent with the exploitation of DDB1, the CRL inhibitory drug MLN4924 (also called Pevonedistat) elicits potent antiviral activity against cytomegaloviruses and several other viruses (21). This is in agreement with the fact that several viral accessory proteins utilize DDB1 and/or CRLs to induce proteasomal degradation of host restriction factors: HIV-1 and HIV-2 encode Vpr, which interacts via VprBP with DDB1 and CRLs and influences processes such as the cell cycle by destabilizing host proteins (11, 12, 23–30). HIV-2 additionally expresses Vpx, which exploits DDB1 and CRLs, also via VprBP, to induce the degradation of SAMHD1 enabling replication in myeloid and dendritic cells (31–37). HBx and WHx, derived from HBV and the Woodchuck hepatitis virus (WHV), respectively, bind DDB1 and CRLs to

induce the degradation of restriction factors such as SMC5/6 (38–42).

We applied immunoprecipitation (IP) coupled to mass spectrometry (MS) to establish a comprehensive and quantitative understanding of the complexes assembled by viral DDB1/CRL-interacting proteins and their targets.

MATERIALS AND METHODS

Cells, Transfection, Infection

Human embryonic kidney (HEK) 293T (ATCC CRL-11268) and mouse NIH3T3 (ATCC CRL-1658) cells obtained from the American Type Culture Collection were used for transfection and infection experiments, respectively. Primary mouse fibroblasts [mouse embryonic fibroblasts [MEF] and mouse newborn cells [MNC]] were isolated from C57BL/6 and BALB/c embryos and newborn mice using protocols described in Le-Trilling and Trilling (43). These animal experiments were approved by local authorities and the corresponding ethics committee (permit number 84-02.04.2014.A390; name of the committee: the Ministry for Environment, Agriculture, Conservation and Consumer Protection of the State of North Rhine-Westphalia in Düsseldorf, Germany; address: LANUV-section 81, Recklinghausen, Germany). Immortalized mouse fibroblasts had been generated from primary C57BL/6 and BALB/c MEF by crisis immortalization (44). All cells were grown in Dulbecco's modified Eagle medium (DMEM) supplemented with 10% (v/v) fetal bovine serum, 100 μ g/ml streptomycin, 100 U/ml penicillin, and 2 mM glutamine. Cell culture media and supplements were obtained from Gibco/Life technologies. The transfection of HEK293T cells was performed by the use of polyethylenimine hydrochloride (PEI, Sigma) at a concentration of 3 μ g PEI/ μ g plasmid DNA. For the infection experiment, recombinant MCMV mutants expressing pM27-HA, pR27-HA, pUL27-HA, or eGFP were used. These mutants were constructed by flp-mediated recombination of an frt-site-flanked fragment—encompassing the human EF1 promoter in front of the respective gene—into a recombinant MCMV bacterial artificial chromosome (BAC) which already harbored an frt-site instead of the M27 sequence. Recombinant MCMVs were reconstituted by transfection of BAC DNA (Superfect, Qiagen) into permissive fibroblasts. For the preparation of MCMV stocks, immortalized MEF were used. Viral titers were determined by standard plaque titration on primary MEF or MNC (43). All infections and virus titrations were done with centrifugal enhancement (800 g for 30 min).

Plasmids

The following expression constructs were used for the IP experiments: pIRES2-EGFP_Intron (BD Biosciences Clontech vector; intron sequence inserted into NheI site in front of the multiple cloning site), pIRES2-EGFP-M27-Flag [described in Trilling et al. (16)], pIRES2-EGFP-M27-HA, pIRES2-EGFP-E27-HA, pIRES2-EGFP-R27-HA, pIRES2-EGFP-UL27-HA, pIRES2-EGFP-Intron-HBx-HA, pIRES2-EGFP-WHx7-HA, pIRES2-EGFP-WHx8-HA, pcDNA-UL42-HA, pcDNA-Vpx-Flag [described in Lim et al. (45)], pcDNA-Vpr-Flag [described in Fregoso et al. (46)], pcDNA-Flag-DDB1 [received from Addgene, described in Hu et al. (47)], and PMZ3F-STAT2-SPA. M27 with a C-terminal HA epitope tag was cloned using the primers KL-M27-1 GAGGGATCCGCCTCTTCGAGGAG and KL-M27-HA2 GAGGGATCCTCAAGCGTAATCTGGAACATC GTATGGGTACACCCGCTCCACCACAACTC to generate a PCR product which was cloned into the BamHI-cleaved pIRES2-EGFP-M27-Flag to exchange the epitope tag. Plasmids containing the coding sequence of the pM27-homologous protein pE27 of the *Murid herpesvirus 8* ("RCMV England") were kindly provided by Sebastian Voigt, Robert-Koch-Institute Berlin and Charité Berlin. The E27 CDS fused to a C-terminal HA epitope tag was subcloned into pIRES2-EGFP by use of the NheI and EcoRI restriction sites. The CDS of pR27 of the *Murid herpesvirus 2* ("RCMV Maastricht") with a C-terminal HA epitope tag was ordered from GeneArt gene synthesis and subcloned into pIRES2-EGFP by NheI and HindIII sites. UL27 of HCMV was cloned by PCR amplification of the CDS using the primers KL-UL27-1 CGGCTAGCATGAACCCCG TGGATCAGCCG and KL-UL27-HA-2 CGGAATTCTCAA GCGTAATCTGGAACATCGTATGGGTATGTGGCGTGACCT CCGACCTC containing restriction sites and a C-terminal HA epitope tag. PCR products were cleaved with NheI and EcoRI and cloned into pIRES-EGFP2. Templates for the PCR amplification of HBx of HBV and the homologous x proteins (termed WHx7 and WHx8) of WHV were kindly provided by Mengji Lu, University of Duisburg-Essen. For the cloning into the expression vectors, primers containing restriction sites and a C-terminal HA epitope tag were used: JR-HBx-1 CGG CTAGCATGGCTGCTAGGCTGTGCTG and JR-HBx-HA-2 CGGAATTCTTAAGCGTAATCTGGAACATCGTATGGGTAG GCAGAGGTGAAAAGTTGCATG for HBx and JR-WHx-1 CGGCTAGCATGGCTGCTCGCCTGTGTTG and JR-WHx-HA-2: CGGAATTCTTAAGCGTAATCTGGAACATCGTATG GGTACAGAAGTCGCATGCATTTATGCC for WHx7 and WHx8. The following primers were used for the cloning of the N-terminal HA tagged HBx: HA-HBx-1 CGGCTAGCATGT ACCCATAACGATGTTCCAGATTACGCTGCTGCTAGGCTGT GCTGCC and HA-HBx-2 CGGAATTCTTAGGCAGAGGTG AAAAAGTTGCATG. PCR products were cleaved with NheI and EcoRI and cloned into pIRES-EGFP2_Intron in the case of HBx and pIRES-EGFP2 in the case of WHx7 and WHx8. pUL42-HA was expressed from pcDNA3.1 (Invitrogen) and was cloned using the following primers: UL42-HA for ATCGTC AAGCTTATGGAGCCCACGCCGATGCTC and UL42-HA rev GACGATGAATTCTTACGCGTAATCTGGAACATCGT ATGGGTACCCCGATGATGCTTGCCT. For the cloning of

pMZ3F-STAT2-SPA, the primers STAT2-SPA for CCTCGAGA TGCGCAGTGGGAAATGCTGC and STAT2-SPA rev GGC GGCCGCAAGTCAGAAGGCATCAAGGGTC were used to generate a PCR product which was cleaved with XhoI and NotI and inserted into the pMZ3F vector (48), which was kindly provided by the lab of Jack Greenblatt, University of Toronto.

Vpr and Vpx, both encoded by HIV-2 (TaxID 11709) Rod-9, expression plasmids were generated by Michael Emerman, Fred Hutchinson Cancer Research Center, and provided to us by Hanna-Mari Baldauf, University Hospital Frankfurt.

HIV-2 Rod10 vpx (49) and HIV-1 M CH106 vpu (50) were cloned via XbaI and MluI restriction sites into bicistronic pCG vectors co-expressing eGFP via an internal ribosome entry site (IRES). The NF- κ B firefly luciferase reporter construct as well as the expression plasmids for p65, a constitutively active mutant of IKK β (S177E, S181E) and dominant negative mutants of IKK α and IKK β were described in Sauter et al. (50) and kindly provided by Bernd Baumann, Ulm University. The pTAL luciferase vector used for normalization was generated by replacing the firefly luciferase gene of a reporter construct purchased from Clontech (# 631909) with a *gaussia* luciferase gene.

Immunoprecipitation

HEK293T cells were washed three times with ice-cold PBS and subsequently lysed by incubation for 1 h on ice in lysis buffer (16). The indicated antibody was added to the supernatant and incubated overnight. Protein-G-sepharose was added and incubated for 1 h. Protein-G-sepharose-bound proteins were washed six times using lysis buffer containing 150–500 mM NaCl. Protein complexes were analyzed by silver-stained SDS-PAGE gels, immunoblotting, or mass spectrometry.

Immunoblotting

Protein and IP samples were separated by classic SDS-PAGE, transferred to nitrocellulose membranes and probed with the following commercially available antibodies: rabbit α -Connexin-43 (Cell Signaling), mouse α -Itch (BD Transduction Laboratories), mouse α -HA (Sigma), rabbit α -HA (Sigma), rabbit α -DDB1 (Bethyl Laboratories Inc), rabbit α -Ncoa5 (Bethyl Laboratories Inc), rabbit α -Xpo7 (Proteintech), mouse α -Flag M2 (Sigma), or mouse α -p65 F6 (Santa Cruz Biotechnology). Xpo7 was also analyzed using an antibody which has been described previously (51) and which was generously provided by Dirk Görlich, Max-Planck Institut f. Biophysikalische Chemie in Göttingen, Germany. After incubation with the appropriate peroxidase-coupled secondary antibodies, signals were visualized with the ECL chemiluminescence system (Cell Signaling).

MS-Based Analysis of Viral Interactomes

For in-gel digestions, 20 μ l of each sample were applied to SDS-PAGE to collect the proteins in a single band for each sample. Protein bands were stained with Coomassie Brilliant Blue and subsequently digested with trypsin (SERVA) overnight at 37°C. Peptides were extracted using 50% (v/v) acetonitrile in 0.1% (v/v) trifluoroacetic acid (TFA) and sonicated twice on ice for 10 min. Extracts were dried by vacuum centrifugation and dissolved in 34 μ l 0.1% (v/v) TFA. The peptide concentration was determined

by quantitative amino acid analysis performed on an ACQUITY-UPLC equipped with AccQ Tag Ultra-UPLC column (Waters). For calibration, Pierce Amino Acid Standard (Thermo Scientific) was used.

Of each sample, 350 ng tryptic peptides were analyzed by LC-ESI-MS/MS on an Orbitrap Elite mass spectrometer online-coupled to an Ultimate 3000 RSLCnano system (both Thermo Scientific). After injection, peptides were trapped on a pre-column (Acclaim PepMap 100, 300 μ m \times 5 mm, C18, 5 μ m, 100 \AA) at a flow rate of 30 μ L/min (0.1% trifluoroacetic acid). After 7 min, peptides were transferred to the analytical column (Acclaim PepMap RSLC, 75 μ m \times 50 cm, nano Viper, C18, 2 μ m, 100 \AA). A 98 min gradient of 5 to 40% of buffer B (0.1% formic acid, 84% acetonitrile) in buffer A (0.1% formic acid) was applied to elute the peptides from the analytical column (flow rate 400 nL/min, column oven temperature 60°C). Full MS spectra were acquired in the Orbitrap analyzer at a mass resolution of 60,000 (mass range 350–2000 m/z). Fragment mass spectra were acquired in data-dependent mode and recorded in the linear ion trap. The twenty most abundant precursor ions were selected for fragmentation using collision-induced dissociation (CID) with a normalized collision energy of 35% and an isolation width of 2.0 m/z.

Protein identification was conducted with Proteome Discoverer software (ver. 1.4.1.14, Thermo Fisher Scientific). Based on the human proteome file UP000005640 downloaded from Uniprot-KB (release 2015_05), a database was constructed containing 68,840 human protein sequences (UniProtKB/Swiss-Prot and UniProtKB/TrEMBL entries) and sequences of eGFP, HA-tagged proteins pM27, HBx, WHx7, WHx8, pR27, pE27, pUL27, pUL42 as well as Flag-tagged proteins Vpr and Vpx. For database searches, Sequest HT algorithm was used as implemented in the respective version of Proteome Discoverer software. Mass tolerance was set to 5 ppm for precursor ions and 0.4 Da for fragment ions. One tryptic miscleavage and variable modifications of methionine (oxidation) and cysteine (propionamide) were allowed. Peptide confidence was estimated using the Target Decoy PSM Validator function implemented in Proteome Discoverer. Peptides with a false discovery rate <1% were considered for analysis. Protein grouping function based on strict maximum parsimony principle was enabled in Proteome Discoverer.

Proteomics data have been deposited to the ProteomeXchange Consortium (<http://proteomecentral.proteomexchange.org>) (52) via the PRIDE partner repository (53) with the data identifier PXD007634 and DOI 10.6019/PXD007634. Files in the mzIdentML standard format were generated using ProCon—PROteomics CONversion tool (ver. 0.9.641) (54).

NF- κ B Promoter Assays

HEK293T cells were co-transfected with an NF- κ B firefly luciferase reporter, a *Gaussia* luciferase construct under the control of a constitutively active pTAL promoter for normalization, and expression vectors for HIV-2 Rod10 Vpx, HIV-1 M CH106 Vpu or dominant negative mutants of IKK α or IKK β . To activate NF- κ B, an expression vector for p65/RelA or a constitutively active mutant of IKK β was co-transfected, or cells

were stimulated with TNF α for 24 h. Two days post-transfection, a dual luciferase assay was performed and the firefly luciferase signals were normalized to the corresponding *Gaussia* luciferase control values.

Statistical Testing

A two-tailed and heteroscedastic (assuming different variances of the compared subpopulations) Student's *t*-Test was used to compare the indicated data sets.

RESULTS

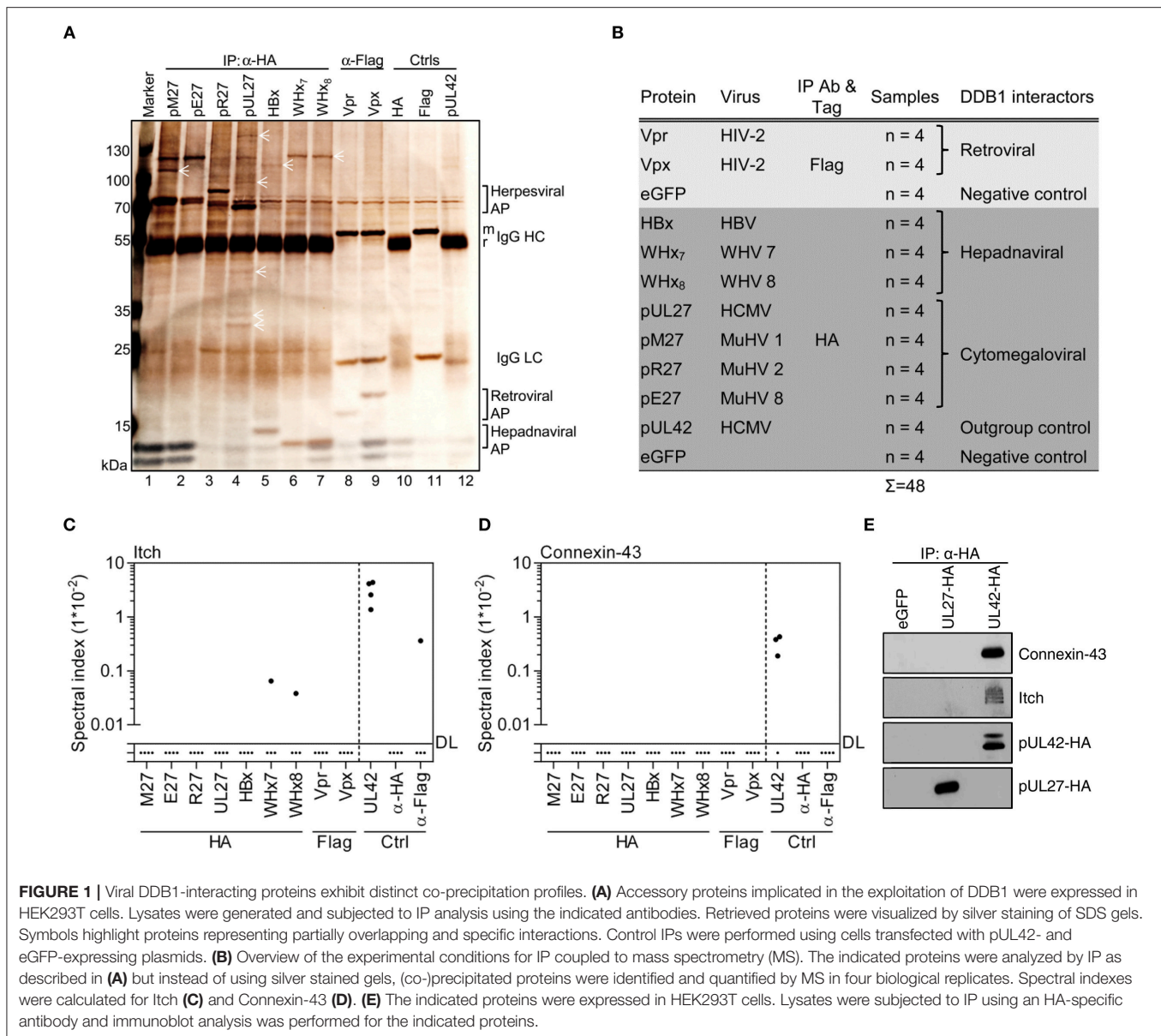
Viral DDB1-Binding Proteins Exhibit Distinct Co-precipitation Profiles

Based on the finding that the HCMV-encoded accessory protein pM27 exploits Cul4A and DDB1 to induce ubiquitination and proteasomal degradation of STAT2, we studied pM27, its HCMV-derived homolog pUL27 as well as pE27 and pR27 of *Murid herpesvirus* (MuHV) 8 and MuHV2, respectively. We further included the DDB1-binding protein HBx of HBV and two WHV homologs derived from genotypes 7 and 8 termed WHx7 and WHx8. Vpr and Vpx encoded by HIV-2 were also included. GFP-expressing cells served as controls. The viral proteins harboring either an HA (pM27, pE27, pR27, pUL27, HBx, WHx7, and WHx8) or a Flag epitope tag (Vpr and Vpx) were expressed in transiently transfected HEK293T cells. After overnight incubation, cells were lysed and subjected to IP using HA- or Flag-specific antibodies, and protein G sepharose, as described in the Material and Methods section. In silver stained SDS-PAGE gels, pM27, pE27, and the WHx proteins interacted with a ~125 kDa protein supposed to be DDB1 (~127 kDa) (**Figure 1A**). Interestingly, no such precipitation was detected in the case of HBx, pUL27, or pR27. Additionally, patterns of specific as well as overlapping interactions became evident.

Since size alone is not a proper way to identify a protein, the immuno-purified complexes were subjected to MS to identify, quantify, and compare the interactomes of these viral accessory proteins (**Figure 1B**). As outlined in more detail below, this comprehensive analysis confirmed previously described interactions, extended known interactions to paralogous host and virus proteins, and identified numerous novel interaction partners.

HCMV-Derived pUL42 Forms a Network of Proteins Harboring WW Domains or PPxY Motifs

In our analyses, we included pUL42 as outgroup control. This HCMV-encoded protein does not recruit DDB1 or CRLs, but interacts with the WW domain of the NEDD4-like Ub ligase Itch via its PPxY motif (55). In agreement with this, pUL42 interacted with Itch (**Figure 1C**) but not with DDB1 or CRL components in our experiments (**Figure S1**). Furthermore, pUL42 retrieved several additional members of the NEDD4 Ub ligase family (NEDD4, NEDD4L, WWP1, and WWP2), known binding partners of NEDD4 Ub ligases (e.g., Connexin-43), other proteins containing WW domains (e.g., YAP1, STXB4,

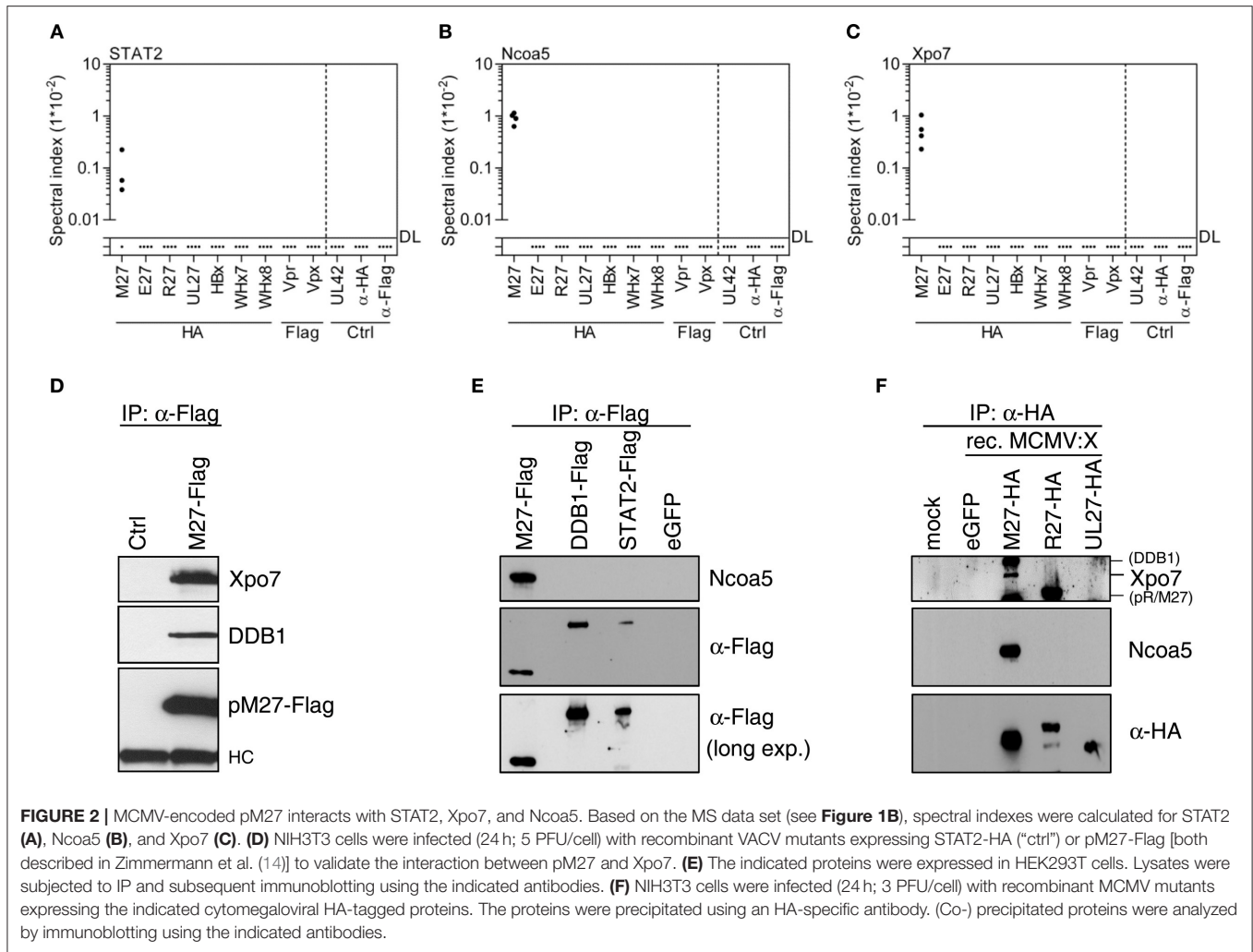


and BAG3), and their interaction partners such as VAMP-2 (**Figure 1D** and **Figures S1, S2**). Notably, Connexin-43 has previously been shown to be downregulated upon HCMV infection (56), and we confirmed its interaction with pUL42 using IP and immunoblotting (**Figure 1E**). Taken together, these data indicate that the HCMV-encoded pUL42 constitutes a suitable outgroup for our approach and reveal that it assembles a protein network most likely bridged through WW domains and corresponding PPxY motifs.

The Interactome of pM27 Supports and Extends the Current Model of pM27 Function

After definition of the outgroup, the interaction network of MCMV pM27 was assessed. As expected from previous

work (16), pM27 efficiently retrieved STAT2 (**Figure 2A**), DDB1, and Cul4A (**Figure S3**). Additionally, several novel interaction partners, including Nco5 and Xpo7, were identified (**Figures 2B,C** and **Figure S3**). Nco5 is an interaction partner of nuclear receptors and exhibits co-activator and co-repressor functions (57, 58). Xpo7 regulates the import and export of several proteins to and from the nucleus (59). Since we had shown before that pM27 precipitates STAT2, DDB1, and Cul4A (14, 16) these herein confirmed interactions strengthen the reliability of our approach. As additional validation, the novel interactions were confirmed by IP and immunoblotting using constructs harboring Flag- instead of HA-epitopes (**Figures 2D,E**). To assess these interactions under infection conditions, we generated recombinant MCMV mutants expressing eGFP or HA epitope-tagged versions of pM27, pR27, or pUL27. In agreement with above experiments,



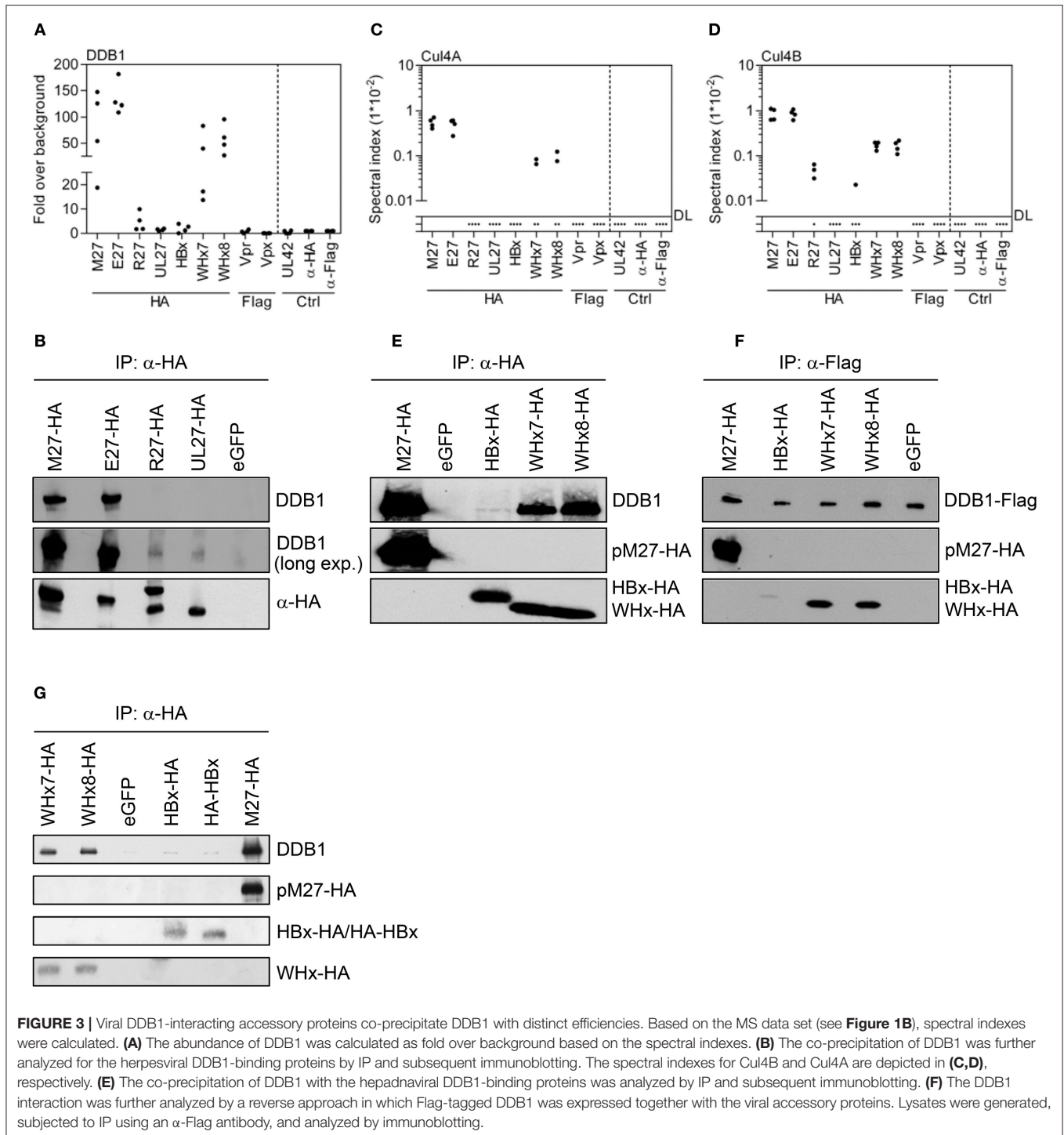
Ncoa5 and Xpo7 exist in complexes with pM27 in MCMV-infected cells (**Figure 2F**), confirming that our MS approach reliably uncovers novel interaction partners of viral accessory proteins.

DDB1-Interacting Viral Accessory Proteins Co-precipitate DDB1 With Distinct Efficiencies

The SDS-PAGE experiments already suggested differences regarding the strength of interaction between viral accessory proteins and DDB1. Consistently, quantitative MS revealed that pM27 retrieved DDB1 ~60-fold more efficiently than pUL27 (**Figure 3A**). The protein pE27 also strongly bound DDB1 (124.9 ± 27.6 -fold over background), whereas the DDB1 interaction was clearly less pronounced in the case of pR27 (3.6 ± 3.4 -fold over background) (**Figure 3A**). These differences were verified by IP and immunoblot analysis (**Figure 3B**). The differential interaction strengths between viral accessory proteins and DDB1 were also recapitulated on the level of Cul4A/B co-precipitation: pM27 and pE27, but not pUL27,

efficiently co-precipitated Cul4A and Cul4B (**Figures 3C,D**). The protein pR27 precipitated Cul4B to a certain extent, albeit clearly less efficient as compared to pM27 and pE27 (**Figure 3D**).

For hepadnaviral HBx and WHx proteins, the interaction with DDB1 is well-described and even substantiated by co-crystallization of DDB1 with synthetic α -helical peptides corresponding to HBx or WHx (39). Consistent with our SDS-PAGE analysis, WHx7 and WHx8 co-precipitated DDB1 very efficiently (**Figure 3A**), whereas HBx only weakly interacted with DDB1 (2.0 ± 1.5 -fold over background; found only in 3 of 4 replicates). WHx7 and WHx8 also precipitated Cul4A and Cul4B, whereas Cul4B was only found in a single HBx IP replicate and Cul4A was not precipitated by HBx at all (**Figures 3C,D**). These differences in DDB1 interaction were substantiated by IP and subsequent immunoblot analysis (**Figure 3E**) and a reverse approach, in which DDB1 was precipitated and HBx, WHx7, and WHx8 were detected (**Figure 3F**). To rule out that the C-terminal HA epitope impairs the interaction between HBx-HA and DDB1, we generated a HBx version harboring an N-terminal HA tag (HA-HBx). However, HA-HBx



and HBx-HA exhibited comparable weak DDB1 interactions (**Figure 3G**). Given the wealth of information on HBx and DDB1 (38, 60–65), the rather weak interaction of HBx with DDB1 and Cul4A/B, especially in contrast to its homologs derived from WHV, was surprising and revealed highly diverse affinities of viral accessory proteins for DDB1, Cul4A, and Cul4B.

Differential Interaction Strengths of Viral Accessory Proteins With DDB1, Cul4A, and Cul4B Suggest a Preference of DDB1 for Cul4B

Interactions of the viral accessory proteins with Cul4A or Cul4B were only detected when DDB1 was also precipitated. The

strength of interaction with DDB1 correlated positively with the retrieval of Cul4A and Cul4B (**Figures S4A,B**), suggesting that the viral proteins primarily recognize DDB1 and co-precipitate Cul4A and Cul4B indirectly via their interaction with DDB1. This is consistent with crystallization and functional data, which show that DDB1 mutations destabilizing the DDB1-Cul4A/B interface abrogate DDB1-dependent effects elicited by HBx (39). As expected, the co-precipitations of Cul4A and Cul4B with the viral accessory proteins showed a highly significant ($p < 0.0001$) positive correlation (**Figure S4C**). The functions of Cul4A and Cul4B are largely overlapping, but discrete functions do also exist (66). DDB1 binds the N-termini of Cul4A and Cul4B. Interestingly, the N-terminus of Cul4B is 149 amino acids longer than that of Cul4A and contains a nuclear localization signal. In all cases and supported by the slope of the linear correlation (0.58 ± 0.03), Cul4B was co-precipitated more efficiently than Cul4A (**Figure S4C**). Taking into account that Cul4A and Cul4B co-precipitated indirectly via DDB1, this argues in favor of a preference of DDB1 for Cul4B as compared to Cul4A.

Confirmation and Extension of Known Interactions of Viral Accessory Proteins

Reitsma et al. determined the interactome of pUL27 and presented a list of 27 precipitated proteins including PSME3, RUVBL2, RUVBL1, and UBR5 (67). Twenty-one of these were also quantified in our study, with 19 precipitating with pUL27. Twelve had spectral indexes above the background precipitation, of which Proteasome activator complex subunit 3 (PSME3; also called PA28 γ), a part of the immune proteasome, was the most prevalent (**Figure 4A** and **Figure S5**). Although PSME3 precipitated to a certain extent in the HA control conditions, the precipitation by pUL27 was 6.89-fold and significantly ($p < 0.03$) above background. Immunoblot experiments confirmed the specific interaction of PSME3 with pUL27 (**Figure 4B**). RUVBL1 and RUVBL2 appeared in the precipitates of most viral accessory proteins and the control settings (**Figure 4C**), suggesting an unspecific retrieval and highlighting the advantage of such comparative experimental designs. DDB1 assembles two different Ub ligase complexes either containing Cul4A/B or the non-CRL Ub ligase UBR5 (28). Several herpesviral proteins interacted with UBR5, confirming the described interaction with pUL27 and extending it to its homologs pM27, pE27, and pR27 (**Figure 4D**). The fact that recruitment of UBR5 is evolutionarily conserved among different herpesviruses suggests a selection advantage of this interaction for viral replication *in vivo*.

Consistent with previous studies (68, 69), HIV-2-derived Vpr co-precipitated VprBP (**Figure S6**). Furthermore, we found an interaction between Bax and Vpr (**Figure 4E**) which is in line with published functional data but has to our knowledge not been experimentally validated before.

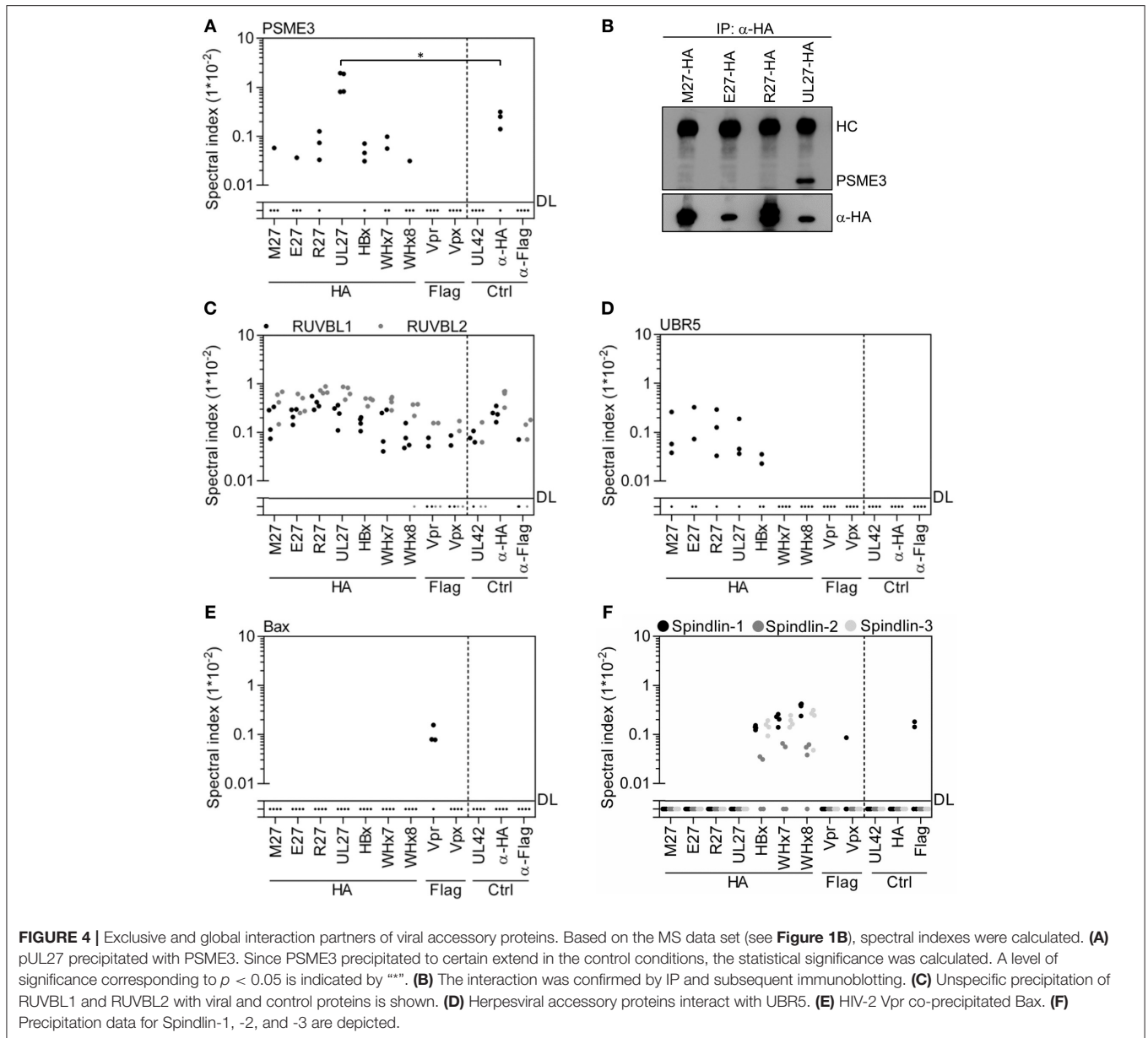
Recently, it was reported that HBx interacts with Spindlin-1 to counteract its inhibition of viral transcription (70). In addition to Spindlin-1, HBx, WHx7, and WHx8 also retrieved its homologs Spindlin-2 and Spindlin-3 (**Figure 4F**). Taken together, our analysis confirmed and significantly extended known or anticipated interactions of viral accessory proteins.

Global Comparison of the Interactomes of Viral DDB1-Interacting Proteins Highlights Overlapping Mechanisms

For a comparison of overlapping and specific interactions of viral accessory proteins with cellular factors according to their phylogeny, we restricted the analysis to interacting proteins found in at least two out of four replicates. Additionally, we compared interactors enriched at least 2-fold above the background (**Figures 5A–C**; numbers in brackets) as well as specific interactors not found in any of the control settings (see red numbers). Tables summarizing the interaction partners of the individual proteins or taxonomic as well as functional groups of viral accessory proteins can be found in the supplementary data (**Supplementary Tables 1–10**). For a systematic overview, we performed a global analysis based on individual correlation coefficients calculated on the spectral indexes of all interactors (**Figure 5D**). Consistent with the existence of a so-called “CRAPome” (71), HA and Flag control IPs correlated positively with each other. Neither the controls nor the outgroup correlated positively with the interactomes of the DDB1/CRL-interacting viral proteins, highlighting the specificity of our approach. The interactomes of the retroviral proteins Vpr and Vpx correlated positively with each other and showed an inverse correlation with the interactomes of the analyzed non-retroviral proteins. The interactomes of the hepadnaviral proteins HBx, WHx7, and WHx8 correlated strongly with each other. This suggests that the global interactomes reflect the phylogenetic relationship of homologous proteins. We also observed a positive correlation between unrelated proteins such as in the case of herpesviral and hepadnaviral proteins (e.g., pM27 and pE27 with WHx) which we interpret as a footprint within the global interactome based on similar functions.

HIV-2 Vpx Co-precipitates p65/RelA and Inhibits NF- κ B-Driven Gene Expression

Within the interactome of Vpx, p65 (also called RelA) was the most abundant specifically interacting protein (**Figure 6A** and **Supplementary Table 10**). Intrigued by the importance of NF- κ B signaling for innate immunity as well as for HIV gene expression, we confirmed this interaction by IP and subsequent immunoblot analysis (**Figure 6B**). Luciferase-based promoter reporter assays were used to investigate the effects of Vpx on NF- κ B-dependent gene expression. NF- κ B was activated at different layers: external stimulation by TNF α , stimulation at the level of the IKK complex by the constitutively active IKK β mutant S177E/S181E, or at the level of p65/RelA by its overexpression. The HIV-1 accessory protein U (Vpu) inhibits NF- κ B upstream of p65/RelA (50) and served as positive control. Consistently, Vpu antagonized NF- κ B signaling induced by TNF α treatment and expression of constitutively active IKK β but not by p65/RelA overexpression (**Figure 6C**). Conversely, Vpx inhibited NF- κ B signaling induced by all stimuli (**Figure 6C**), indicating that Vpx directly acts on p65/RelA. As expected, Vpx inhibits RelA/p65-induced NF- κ B activation in a dose-dependent manner (**Figure 6D**). Since NF- κ B signal transduction relies

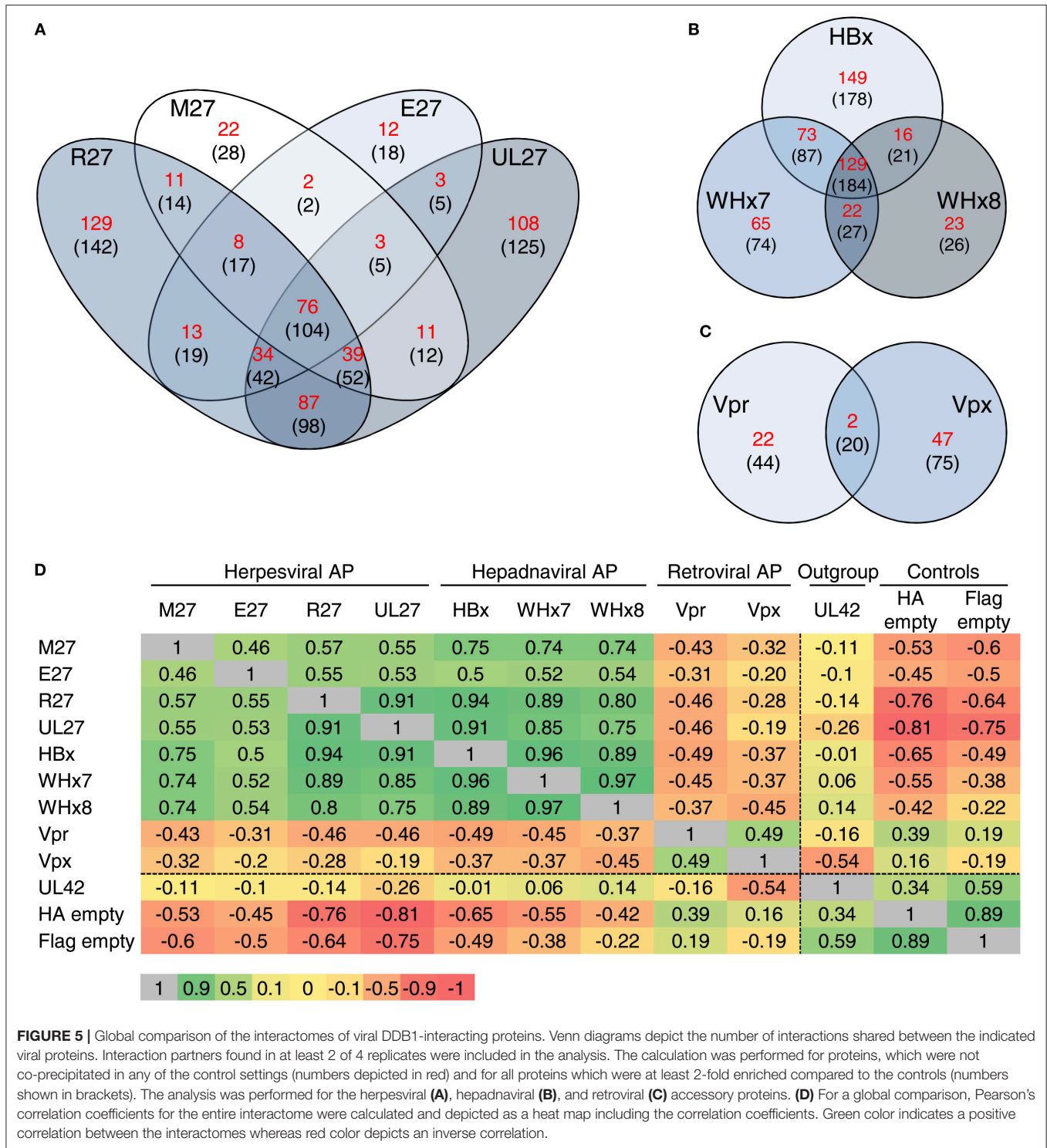


on the β -TrCP/Skp1/Cullin1 complex for $\text{I}\kappa\text{B}\alpha$ degradation, inhibitors such as MG132 cannot be used to elucidate Ub ligase-dependency of Vpx-mediated NF- κ B inhibition. Therefore, the Vpx mutant Q76A, known to lack the ability to interact with VprBP and DDB1 (32), was used to test the relevance of CRLs (**Figure 6E**). The results suggest that the interaction with DDB1 and CRLs significantly contributes to the NF- κ B inhibitory activity of Vpx, although we cannot exclude that the Q76A mutation has pleiotropic effects on Vpx. To test if the interaction of Vpx with DDB1 and RelA/p65 results in the degradation of RelA/p65, we performed co-transfection experiments with Vpx and RelA/p65 expression plasmids. The experiments were conducted in the presence or absence of MG132. MG132 did not change the RelA/p65 abundance, irrespective of the presence of Vpx, and we did not observe decreased RelA/p65 amounts in the

presence of Vpx (data not shown). We infected lymphocytes with Vpx-positive and Vpx-negative HIV-2 viruses, and determined RelA/p65 by flow cytometry. Also under these conditions, we did not observe significant changes in the RelA/p65 abundance in the presence of Vpx (data not shown). We hypothesize that Vpx-mediated inhibition of NF- κ B signaling cannot be explained sufficiently by proteasomal degradation of RelA/p65. Taken together, our determination of the interactomes of viral accessory proteins uncovered novel interactions with biological relevance.

DISCUSSION

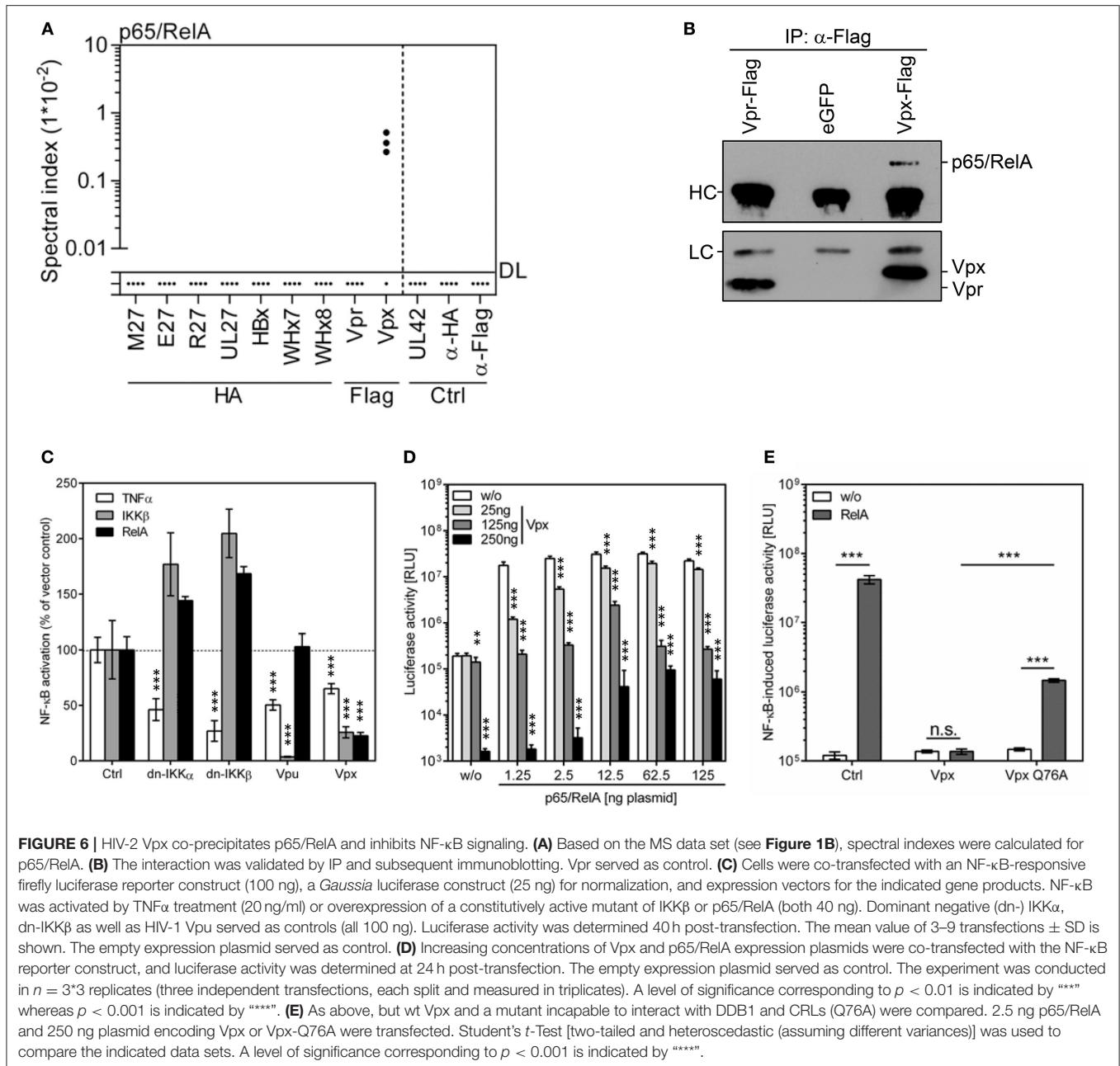
Viruses frequently dismantle cell intrinsic immunity by evolving accessory proteins that bridge antiviral factors to proteins



inducing proteolysis, e.g., DDB1 and CRLs or other components of the Ub proteasome pathway. Since CRLs became amenable for pharmacologic intervention using drugs such as MLN4924 and since CRL activity is essential for replication of several human-pathogenic viruses (21, 72), viral CRL exploitation may be turned into therapeutic approaches. Understanding the

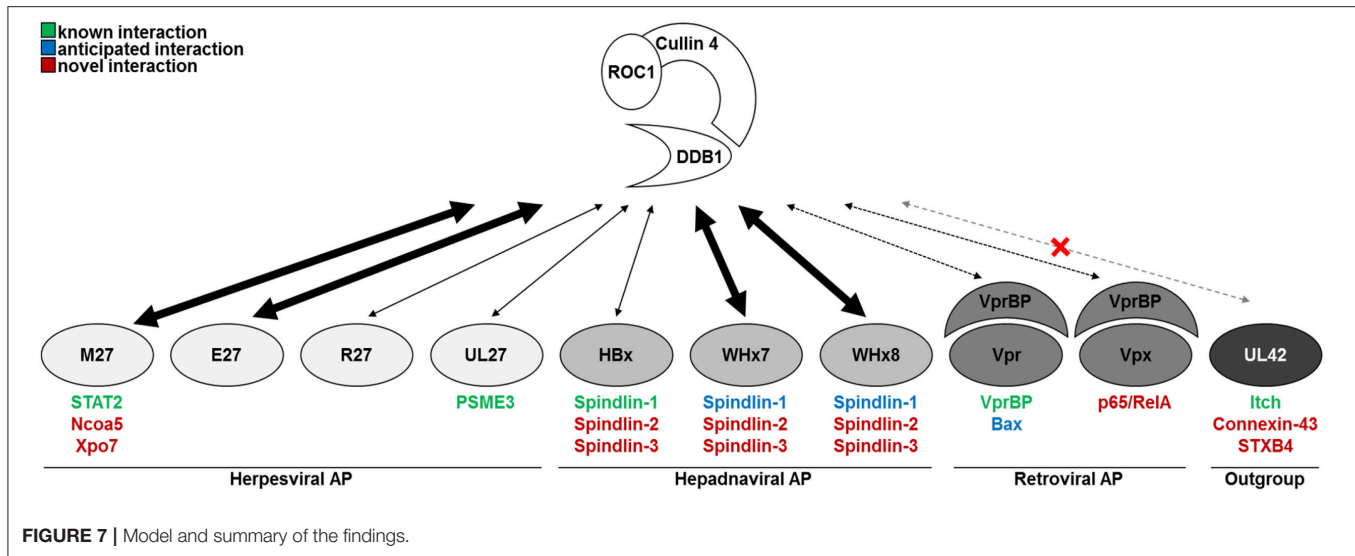
exact mechanisms and interactomes of viral accessory proteins might uncover additional and more specific Achilles' heels of viruses.

Here, we comprehensively compared the interactomes of nine viral accessory proteins known or suspected to interact with DDB1 and/or CRLs and of one outgroup control protein,



which did not interact with CRLs but with other Ub ligases of the NEDD4 family (Figure 7). We found that the strength of the interaction between the herpes-, hepadna-, and retroviral accessory proteins and DDB1 and/or CRLs was remarkably different. Despite the fact that the interaction between HBx and DDB1 was confirmed by the co-crystallization of full-length DDB1 with short α -helical peptides corresponding to HBx (39), the interaction turned out to be surprisingly weak in comparison to WHx7, WHx8, pE27, and pM27. This functional difference between HBx and WHx is supported by the existing crystal structure data: the superposition of the DDB1-HBx and DDB1-WHx structures shows that three strong hydrogen

bonds are formed between the N-terminal part of WHx and the cognate 4b–4c loop of DDB1, whereas the DDB1 loop is pushed further out in the DDB1-HBx heterodimer only allowing weaker hydrophobic and van der Waals interactions. What might be the reason for this difference? Recent findings documented the existence of stimulatory functions of DDB1 on HBV transcription by HBx-dependent as well as independent mechanisms (73). It is tempting to speculate that the strength of interaction between HBx and DDB1 might represent a virus-specific trade-off between direct effects and HBx-independent functions. Additionally, DDB1 is essential for cell proliferation and survival (74, 75) and some DDB1 functions are impaired



by HBx, leading to cell death (76, 77). This suggests that the association between viral accessory proteins and DDB1 needs to balance advantageous and disadvantageous consequences—presumably in a virus-specific manner.

HBx was also shown to interact with Spindlin-1 to alleviate its antiviral effects against HBV (and *Herpesviridae*) (70). We confirmed this interaction and extended it to the WHV-expressed homologs WHx7 and WHx8, indicating evolutionary conservation and functional relevance *in vivo*. Previously described anti- and proviral effects of Spindlin-1 overexpression and siRNA-mediated ablation, respectively, were statistically significant but moderate (below $1 \times \log_{10}$) (70). Our finding that HBx and WHx also interact with Spindlin-2 and Spindlin-3 suggests redundancy in this recently identified intrinsic defense system.

In addition to hepadnaviral proteins, we also included two lentiviral proteins (i.e., HIV-2 Vpr and Vpx) in our analyses. While HIV-1 Vpr-induced apoptosis occurs in a Bax-dependent manner (78), a direct physical interaction of these two proteins was to our knowledge never substantiated experimentally. The herein shown co-precipitation with HIV-2 Vpr extends the finding from HIV-1 to HIV-2 and fills this gap concerning the physical interaction.

To enable a comparative analysis of the interactomes of the different viral proteins, one cell line was used throughout all experiments. Due to their ubiquitous availability and broad application, we selected HEK293T cells for this purpose. One might argue that viral accessory proteins will usually be expressed in other cell types (e.g., HIV-encoded proteins in CD4+ T lymphocytes or macrophages) and that this experimental approach constitutes a potential confounding factor of our data set. However, HIV can efficiently replicate in HEK293 cells once CD4 expression is enforced (79), suggesting suitability for studies addressing intracellular protein-protein interactions. This is in conjunction with the fact that we confirmed numerous known interactions and were able to validate newly

identified interactions under infection conditions (see e.g., Figure 2F).

As a proof of principle for the relevance of the newly identified interactions, we studied the functional consequences of the interaction between HIV-2 Vpx and p65/RelA. Based on the presence of RelA in the Vpx interactome, we tested if Vpx influences NF- κ B signal transduction and found that Vpx efficiently inhibited NF- κ B activation. To identify the step of the signaling cascade that is targeted by Vpx, we activated NF- κ B signaling using different stimuli. Vpx antagonizes NF- κ B signaling stimulated by TNF α treatment, expression of constitutively active IKK β as well as RelA overexpression. Especially the latter result strongly suggests that the interaction between Vpx and RelA is indeed functionally relevant. NF- κ B signaling is crucial for the induction and regulation of innate, adaptive, and intrinsic immune responses. Consistently, numerous viruses express proteins, which modulate NF- κ B signaling (80). In case of HIV-1 and HIV-2, the situation is complicated by the fact that both viruses contain functional NF- κ B binding sites in their LTR promoters which are highly relevant for viral gene expression and replication (81)—although they seem not to be absolutely essential for viral growth (82). It may appear counterintuitive that a virus, which exploits NF- κ B sites in its promoter and which exploits NF- κ B signaling for its own transcription, should express an antagonist targeting RelA. However, NF- κ B inhibitory effects are clearly documented for the accessory proteins Vpu and Vpr of HIV-1 and related primate lentiviruses (50, 83–87). These NF- κ B inhibitory activities may confer a selection advantage as they prevent the NF- κ B-driven expression of anti-viral cytokines [e.g., IFNs and Rantes (83)] and restriction factors during late stages of the viral replication cycle when efficient expression of viral genes has already been initiated.

Taken together, our comparative study on the interactome of viral accessory proteins known or suspected to interact with DDB1 and CRLs uncovered several new aspects of the biology of these important proteins. Furthermore, our data constitute a rich

resource for future studies addressing the molecular functions and mechanisms of these viral proteins.

DATA AVAILABILITY STATEMENT

The proteomic datasets generated for this study can be found in the ProteomeXchange Consortium (<http://proteomecentral.proteomexchange.org>) (52) via the PRIDE partner repository (53) with the data identifier PXD007634 and DOI 10.6019/PXD007634.

AUTHOR CONTRIBUTIONS

CL, MR, ME, JR-A, SeH, StH, and VTKL-T did experiments. DM and BS performed MS quantifications. DH and DS analyzed the effect of HIV-2 Vpx on NF- κ B activation. CL, VTKL-T, and MT wrote the paper. VTKL-T and MT supervised the project.

FUNDING

VTKL-T, DS, BS, and MT receive funding from the DFG (TRR60, SPP1923, and GRK1949). MT received support by

the Medical Faculty Essen (IFORES program for innovative research) and BS by P.U.R.E (Protein research Unit Ruhr within Europe; 233-1.08.03.03-031-68079). DH was supported by the International Graduate School in Molecular Medicine Ulm (IGradU).

ACKNOWLEDGMENTS

We thank Hanna-Mari Baldauf (University Hospital Frankfurt), Michael Emerman (Fred Hutchinson Cancer Research Center), Mengji Lu (University Duisburg Essen), Bernd Baumann (Ulm University, Germany), and Sebastian Voigt (RKI and Charité Berlin) for generously providing reagents. pcDNA-FLAG-DDB1 was a gift from Yue Xiong (Addgene plasmid # 19918).

SUPPLEMENTARY MATERIAL

The Supplementary Material for this article can be found online at: <https://www.frontiersin.org/articles/10.3389/fimmu.2018.02978/full#supplementary-material>

REFERENCES

- Trilling M, Bellora N, Rutkowski AJ, De Graaf M, Dickinson P, Robertson K, et al. Deciphering the modulation of gene expression by type I and II interferons combining 4sU-tagging, translational arrest and *in silico* promoter analysis. *Nucleic Acids Res.* (2013) 41:8107–25. doi: 10.1093/nar/gkt589
- Megger DA, Philipp J, Le-Trilling VTK, Sitek B, Trilling M. Deciphering of the human interferon-regulated proteome by mass spectrometry-based quantitative analysis reveals extent and dynamics of protein induction and repression. *Front Immunol.* (2017) 8:1139. doi: 10.3389/fimmu.2017.01139
- Duggal NK, Emerman M. Evolutionary conflicts between viruses and restriction factors shape immunity. *Nat Rev Immunol.* (2012) 12:687–95. doi: 10.1038/nri3295
- Rock KL, Gramm C, Rothstein L, Clark K, Stein R, Dick L, et al. Inhibitors of the proteasome block the degradation of most cell proteins and the generation of peptides presented on MHC class I molecules. *Cell* (1994) 78:761–71.
- Hershko A, Ciechanover A. The ubiquitin system. *Ann Rev Biochem.* (1998) 67:425–79.
- Barry M, Fruh K. Viral modulators of cullin RING ubiquitin ligases: culling the host defense. *Sci STKE* (2006) 2006:pe21. doi: 10.1126/stke.3352006pe21
- Gustin JK, Moses AV, Fruh K, Douglas JL. Viral takeover of the host ubiquitin system. *Front Microbiol.* (2011) 2:161. doi: 10.3389/fmicb.2011.00161
- Kaspari M, Tavalai N, Stamminger T, Zimmermann A, Schilf R, Bogner E. Proteasome inhibitor MG132 blocks viral DNA replication and assembly of human cytomegalovirus. *FEBS Lett.* (2008) 582:666–72. doi: 10.1016/j.febslet.2008.01.040
- Dudek SE, Luig C, Pauli EK, Schubert U, Ludwig S. The clinically approved proteasome inhibitor PS-341 efficiently blocks influenza A virus and vesicular stomatitis virus propagation by establishing an antiviral state. *J Virol.* (2010) 84:9439–51. doi: 10.1128/JVI.00533-10
- Mercer J, Snijder B, Sacher R, Burkard C, Bleck CK, Stahlberg H, et al. RNAi screening reveals proteasome- and Cullin3-dependent stages in vaccinia virus infection. *Cell Rep.* (2012) 2:1036–47. doi: 10.1016/j.celrep.2012.09.003
- Romani B, Shaykh Baygloo N, Aghasadeghi MR, Allahbakhshi E. HIV-1 Vpr protein enhances proteasomal degradation of MCM10 DNA replication factor through the Cul4-DDB1[VprBP] E3 ubiquitin ligase to induce G2/M cell cycle arrest. *J Biol Chem.* (2015) 290:17380–9. doi: 10.1074/jbc.M115.641522
- Romani B, Baygloo NS, Hamidi-Fard M, Aghasadeghi MR, Allahbakhshi E. HIV-1 Vpr protein induces proteasomal degradation of chromatin-associated class I HDACs to overcome latent infection of macrophages. *J Biol Chem.* (2016) 291:2696–711. doi: 10.1074/jbc.M115.689018
- Yen HC, Xu Q, Chou DM, Zhao Z, Elledge SJ. Global protein stability profiling in mammalian cells. *Science* (2008) 322:918–23. doi: 10.1126/science.1160489
- Zimmermann A, Trilling M, Wagner M, Wilborn M, Bubic I, Jonjic S, et al. A cytomegaloviral protein reveals a dual role for STAT2 in IFN- γ signaling and antiviral responses. *J Exp Med.* (2005) 201:1543–53. doi: 10.1084/jem.20041401
- Le VTK, Trilling M, Wilborn M, Hengel H, Zimmermann A. Human cytomegalovirus interferes with signal transducer and activator of transcription (STAT) 2 protein stability and tyrosine phosphorylation. *J Gen Virol.* (2008) 89:2416–26. doi: 10.1099/vir.0.2008/001669-0
- Trilling M, Le VTK, Fiedler M, Zimmermann A, Bleifuss E, Hengel H. Identification of DNA-damage DNA-binding protein 1 as a conditional essential factor for cytomegalovirus replication in interferon-gamma-stimulated cells. *PLoS Pathog.* (2011) 7:e1002069. doi: 10.1371/journal.ppat.1002069
- Trilling M, Le VTK, Hengel H. Interplay between CMVs and interferon signaling: implications for pathogenesis and therapeutic intervention. *Fut Microbiol.* (2012) 7:1269–82. doi: 10.2217/fmb.12.109
- Trilling M, Le VTK, Rashidi-Alavijeh J, Katschinski B, Scheller J, Rose-John S, et al. “Activated” STAT proteins: a paradoxical consequence of inhibited JAK-STAT signaling in cytomegalovirus-infected cells. *J Immunol.* (2014) 192:447–58. doi: 10.4049/jimmunol.1203516
- Le-Trilling VTK, Trilling M. Attack, parry and riposte: molecular fencing between the innate immune system and human herpesviruses. *Tissue Antigens* (2015) 86:1–13. doi: 10.1111/tan.12594
- Le-Trilling VTK, Wohlgemuth K, Ruckborn MU, Jagnjic A, Maassen F, Timmer L, et al. STAT2-dependent immune responses ensure host survival despite the presence of a potent viral antagonist. *J Virol.* (2018) 92:1–17. doi: 10.1128/JVI.00296-18
- Le-Trilling VTK, Megger DA, Katschinski B, Landsberg CD, Ruckborn MU, Tao S, et al. Broad and potent antiviral activity of the NAE inhibitor MLN4924. *Sci Rep.* (2016) 6:19977. doi: 10.1038/srep19977
- Iovine B, Iannella ML, Bevilacqua MA. Damage-specific DNA binding protein 1 (DDB1): a protein with a wide range of functions. *Int J Biochem Cell Biol.* (2011) 43:1664–7. doi: 10.1016/j.biocel.2011.09.001

23. Belzile JP, Duisit G, Rougeau N, Mercier J, Finzi A, Cohen EA. HIV-1 Vpr-mediated G2 arrest involves the DDB1-CUL4AVPRBP E3 ubiquitin ligase. *PLoS Pathog.* (2007) 3:e85. doi: 10.1371/journal.ppat.0030085
24. Hrecka K, Gierszewska M, Srivastava S, Kozaczekiewicz L, Swanson SK, Florens L, et al. Lentiviral Vpr usurps Cul4-DDB1[VprBP] E3 ubiquitin ligase to modulate cell cycle. *Proc Natl Acad Sci USA.* (2007) 104:11778–83. doi: 10.1073/pnas.0702102104
25. Tan L, Ehrlich E, Yu XF. DDB1 and Cul4A are required for human immunodeficiency virus type 1 Vpr-induced G2 arrest. *J Virol.* (2007) 81:10822–30. doi: 10.1128/JVI.01380-07
26. Ahn J, Vu T, Novince Z, Guerrero-Santoro J, Rapic-Otrin V, Gronenborn AM. HIV-1 Vpr loads uracil DNA glycosylase-2 onto DCAF1, a substrate recognition subunit of a cullin 4A-ring E3 ubiquitin ligase for proteasome-dependent degradation. *J Biol Chem.* (2010) 285:37333–41. doi: 10.1074/jbc.M110.133181
27. Huang CY, Chiang SF, Lin TY, Chiou SH, Chow KC. HIV-1 Vpr triggers mitochondrial destruction by impairing Mfn2-mediated ER-mitochondria interaction. *PLoS ONE* (2012) 7:e33657. doi: 10.1371/journal.pone.0033657
28. Wang X, Singh S, Jung HY, Yang G, Jun S, Sastry KJ, et al. HIV-1 Vpr protein inhibits telomerase activity via the EDD-DDB1-VPRBP E3 ligase complex. *J Biol Chem.* (2013) 288:15474–80. doi: 10.1074/jbc.M112.416735
29. Laguette N, Bregnard C, Hue P, Basbous J, Yatim A, Larroque M, et al. Premature activation of the SLX4 complex by Vpr promotes G2/M arrest and escape from innate immune sensing. *Cell* (2014) 156:134–45. doi: 10.1016/j.cell.2013.12.011
30. Lahouassa H, Blondot ML, Chauveau L, Chougui G, Morel M, Leduc M, et al. HIV-1 Vpr degrades the HLTf DNA translocase in T cells and macrophages. *Proc Natl Acad Sci USA.* (2016) 113:5311–6. doi: 10.1073/pnas.1600485113
31. Sharova N, Wu Y, Zhu X, Stranska R, Kaushik R, Sharkey M, et al. Primate lentiviral Vpx commandeers DDB1 to counteract a macrophage restriction. *PLoS Pathog.* (2008) 4:e1000057. doi: 10.1371/journal.ppat.1000057
32. Srivastava S, Swanson SK, Manel N, Florens L, Washburn MP, Skowronski J. Lentiviral Vpx accessory factor targets VprBP/DCAF1 substrate adaptor for cullin 4 E3 ubiquitin ligase to enable macrophage infection. *PLoS Pathog.* (2008b) 4:e1000059. doi: 10.1371/journal.ppat.1000059
33. Hrecka K, Hao C, Gierszewska M, Swanson SK, Kesik-Brodacka M, Srivastava S, et al. Vpx relieves inhibition of HIV-1 infection of macrophages mediated by the SAMHD1 protein. *Nature* (2011) 474:658–61. doi: 10.1038/nature10195
34. Laguette N, Sobhian B, Casartelli N, Ringgaard M, Chable-Bessia C, Segal E, et al. SAMHD1 is the dendritic- and myeloid-cell-specific HIV-1 restriction factor counteracted by Vpx. *Nature* (2011) 474:654–7. doi: 10.1038/nature10117
35. Ahn J, Hao C, Yan J, Delucia M, Mehrens J, Wang C, et al. HIV/simian immunodeficiency virus (SIV) accessory virulence factor Vpx loads the host cell restriction factor SAMHD1 onto the E3 ubiquitin ligase complex CRL4DCAF1. *J Biol Chem.* (2012) 287:12550–8. doi: 10.1074/jbc.M112.340711
36. Wei W, Guo H, Gao Q, Markham R, Yu XF. Variation of two primate lineage-specific residues in human SAMHD1 confers resistance to N terminus-targeted SIV Vpx proteins. *J Virol.* (2014a) 88:583–91. doi: 10.1128/JVI.02866-13
37. Wei W, Guo H, Liu X, Zhang H, Qian L, Luo K, et al. A first-in-class NAE inhibitor, MLN4924, blocks lentiviral infection in myeloid cells by disrupting neddylation-dependent Vpx-mediated SAMHD1 degradation. *J Virol.* (2014b) 88:745–51. doi: 10.1128/JVI.02568-13
38. Becker SA, Lee TH, Butel JS, Slagle BL. Hepatitis B virus X protein interferes with cellular DNA repair. *J Virol.* (1998) 72:266–72.
39. Li T, Robert EI, Van Breugel PC, Strubin M, Zheng N. A promiscuous alpha-helical motif anchors viral hijackers and substrate receptors to the CUL4-DDB1 ubiquitin ligase machinery. *Nat Struct Mol Biol.* (2010) 17:105–11. doi: 10.1038/nsmb.1719
40. Van Breugel PC, Robert EI, Mueller H, Decorsiere A, Zoulim F, Hantz O, et al. Hepatitis B virus X protein stimulates gene expression selectively from extrachromosomal DNA templates. *Hepatology* (2012) 56:2116–24. doi: 10.1002/hep.25928
41. Decorsiere A, Mueller H, Van Breugel PC, Abdul F, Gerossier L, Beran RK, et al. Hepatitis B virus X protein identifies the Smc5/6 complex as a host restriction factor. *Nature* (2016) 531:386–9. doi: 10.1038/nature17170
42. Murphy CM, Xu Y, Li F, Nio K, Reszka-Blanco N, Li X, et al. Hepatitis B virus X protein promotes degradation of SMC5/6 to enhance HBV replication. *Cell Rep.* (2016) 16:2846–54. doi: 10.1016/j.celrep.2016.08.026
43. Le-Trilling VTK, Trilling M. Mouse newborn cells allow highly productive mouse cytomegalovirus replication, constituting a novel convenient primary cell culture system. *PLoS ONE* (2017) 12:e0174695. doi: 10.1371/journal.pone.0174695
44. Rattay S, Trilling M, Megger DA, Sitek B, Meyer HE, Hengel H, et al. The Canonical immediate early 3 gene product pIE611 of mouse cytomegalovirus is dispensable for viral replication but mediates transcriptional and posttranscriptional regulation of viral gene products. *J Virol.* (2015) 89:8590–8. doi: 10.1128/JVI.01234-15
45. Lim ES, Fregoso OI, McCoy CO, Matsen FA, Malik HS, Emerman M. The ability of primate lentiviruses to degrade the monocyte restriction factor SAMHD1 preceded the birth of the viral accessory protein Vpx. *Cell Host Microbe* (2012) 11:194–204. doi: 10.1016/j.chom.2012.01.004
46. Fregoso OI, Emerman M. Activation of the DNA damage response is a conserved function of HIV-1 and HIV-2 Vpr that is independent of SLX4 recruitment. *MBio* (2016) 7:1–10. doi: 10.1128/mBio.01433-16
47. Hu J, Zacharek S, He YJ, Lee H, Shumway S, Duronio RJ, et al. WD40 protein FBW5 promotes ubiquitination of tumor suppressor TSC2 by DDB1-CUL4-ROC1 ligase. *Genes Dev.* (2008) 22:866–71. doi: 10.1101/gad.1624008
48. Zeghouf M, Li J, Butland G, Borkowska A, Canadien V, Richards D, et al. Sequential Peptide Affinity (SPA) system for the identification of mammalian and bacterial protein complexes. *J Proteome Res.* (2004) 3:463–8. doi: 10.1021/pr034084x
49. Yu H, Usmani SM, Borch A, Kramer J, Sturzel CM, Khalid M, et al. The efficiency of Vpx-mediated SAMHD1 antagonism does not correlate with the potency of viral control in HIV-2-infected individuals. *Retrovirology* (2013) 10:27. doi: 10.1186/1742-4690-10-27
50. Sauter D, Hotter D, Van Driessche B, Sturzel CM, Kluge SF, Wildum S, et al. Differential regulation of NF-kappaB-mediated proviral and antiviral host gene expression by primate lentiviral Nef and Vpu proteins. *Cell Rep.* (2015) 10:586–99. doi: 10.1016/j.celrep.2014.12.047
51. Mingot JM, Bohnsack MT, Jakle U, Gorlich D. Exportin 7 defines a novel general nuclear export pathway. *EMBO J.* (2004) 23:3227–36. doi: 10.1038/sj.emboj.7600338
52. Vizcaino JA, Deutsch EW, Wang R, Csordas A, Reisinger F, Rios D, et al. ProteomeXchange provides globally coordinated proteomics data submission and dissemination. *Nat Biotechnol.* (2014) 32:223–6. doi: 10.1038/nbt.2839
53. Vizcaino JA, Cote RG, Csordas A, Dianas JA, Fabregat A, Foster JM, et al. The PRoteomics IDentifications (PRIDE) database and associated tools: status in 2013. *Nucleic Acids Res.* (2013) 41:D1063–9. doi: 10.1093/nar/gks1262
54. Mayer G, Stephan C, Meyer HE, Kohl M, Marcus K, Eisenacher M. ProCon - proteomics conversion tool. *J Proteomics* (2015) 129:56–62. doi: 10.1016/j.jprot.2015.06.015
55. Koshizuka T, Tanaka K, Suzutani T. Degradation of host ubiquitin E3 ligase Itch by human cytomegalovirus UL42. *J Gen Virol.* (2016) 97:196–208. doi: 10.1099/jgv.0.000336
56. Stanton RJ, Mcsharry BP, Rickards CR, Wang EC, Tomasec P, Wilkinson GW. Cytomegalovirus destruction of focal adhesions revealed in a high-throughput Western blot analysis of cellular protein expression. *J Virol.* (2007) 81:7860–72. doi: 10.1128/JVI.02247-06
57. Sauve F, Mcbroom LD, Gallant J, Moraitis AN, Labrie F, Giguere V. CIA, a novel estrogen receptor coactivator with a bifunctional nuclear receptor interacting determinant. *Mol Cell Biol.* (2001) 21:343–53. doi: 10.1128/MCB.21.1.343-353.2001
58. Gillespie MA, Gold ES, Ramsey SA, Podolsky I, Aderem A, Ranish JA. An LXR-NCOA5 gene regulatory complex directs inflammatory crosstalk-dependent repression of macrophage cholesterol efflux. *EMBO J.* (2015) 34:1244–58. doi: 10.15252/embj.201489819
59. Aksu M, Pleiner T, Karaca S, Kappert C, Dehne HJ, Seibel K, et al. Xpo7 is a broad-spectrum exportin and a nuclear import receptor. *J Cell Biol.* (2018) 217:2329–40. doi: 10.1083/jcb.201712013
60. Sitterlin D, Bergametti F, Transy C. UVDDDB p127-binding modulates activities and intracellular distribution of hepatitis B virus X protein. *Oncogene* (2000) 19:4417–26. doi: 10.1038/sj.onc.1203771

61. Wentz MJ, Becker SA, Slagle BL. Dissociation of DDB1-binding and transactivation properties of the hepatitis B virus X protein. *Virus Res.* (2000) 68:87–92. doi: 10.1016/S0168-1702(00)00160-X
62. Bergametti F, Sitterlin D, Transy C. Turnover of hepatitis B virus X protein is regulated by damaged DNA-binding complex. *J Virol.* (2002) 76:6495–501. doi: 10.1128/JVI.76.13.6495-6501.2002
63. Leupin O, Bontron S, Strubin M. Hepatitis B virus X protein and simian virus 5V protein exhibit similar UV-DDB1 binding properties to mediate distinct activities. *J Virol.* (2003) 77:6274–83. doi: 10.1128/JVI.77.11.6274-6283.2003
64. Guo L, Wang X, Ren L, Zeng M, Wang S, Weng Y, et al. HBx affects CUL4-DDB1 function in both positive and negative manners. *Biochem Biophys Res Commun.* (2014) 450:1492–7. doi: 10.1016/j.bbrc.2014.07.019
65. Minor MM, Slagle BL. Hepatitis B virus HBx protein interactions with the ubiquitin proteasome system. *Viruses* (2014) 6:4683–702. doi: 10.3390/v6114683
66. Hannah J, Zhou P. Distinct and overlapping functions of the cullin E3 ligase scaffolding proteins CUL4A and CUL4B. *Gene* (2015) 573:33–45. doi: 10.1016/j.gene.2015.08.064
67. Reitsma JM, Savaryn JP, Faust K, Sato H, Halligan BD, Terhune SS. Antiviral inhibition targeting the HCMV kinase pUL97 requires pUL27-dependent degradation of Tip60 acetyltransferase and cell-cycle arrest. *Cell Host Microbe* (2011) 9:103–14. doi: 10.1016/j.chom.2011.01.006
68. Zhao LJ, Mukherjee S, Narayan O. Biochemical mechanism of HIV-1 Vpr function. Specific interaction with a cellular protein. *J Biol Chem.* (1994) 269:15577–82.
69. Zhang S, Feng Y, Narayan O, Zhao LJ. Cytoplasmic retention of HIV-1 regulatory protein Vpr by protein-protein interaction with a novel human cytoplasmic protein VprBP. *Gene* (2001) 263:131–40. doi: 10.1016/S0378-1119(00)00583-7
70. Ducroux A, Benhenda S, Riviere L, Semmes OJ, Benkirane M, Neuveut C. The Tudor domain protein Spindlin1 is involved in intrinsic antiviral defense against incoming hepatitis B Virus and herpes simplex virus type 1. *PLoS Pathog.* (2014) 10:e1004343. doi: 10.1371/journal.ppat.1004343
71. Mellacheruvu D, Wright Z, Couzens AL, Lambert JR, St-Denis NA, Li T, et al. The CRAPome: a contaminant repository for affinity purification-mass spectrometry data. *Nat Methods* (2013) 10:730–6. doi: 10.1038/nmeth.2557
72. Nekorchuk MD, Sharifi HJ, Furuya AK, Jellinger R, De Noronha CM. HIV relies on neddylation for ubiquitin ligase-mediated functions. *Retrovirology* (2013) 10:138. doi: 10.1186/1742-4690-10-138
73. Kim W, Lee S, Son Y, Ko C, Ryu WS. DDB1 Stimulates Viral Transcription of Hepatitis B Virus via HBx-Independent Mechanisms. *J Virol.* (2016) 90:9644–53. doi: 10.1128/JVI.00977-16
74. Cang Y, Zhang J, Nicholas SA, Bastien J, Li B, Zhou P, et al. Deletion of DDB1 in mouse brain and lens leads to p53-dependent elimination of proliferating cells. *Cell* (2006) 127:929–40. doi: 10.1016/j.cell.2006.09.045
75. Cang Y, Zhang J, Nicholas SA, Kim AL, Zhou P, Goff SP. DDB1 is essential for genomic stability in developing epidermis. *Proc Natl Acad Sci USA.* (2007) 104:2733–7. doi: 10.1073/pnas.0611311104
76. Bontron S, Lin-Marq N, Strubin M. Hepatitis B virus X protein associated with UV-DDB1 induces cell death in the nucleus and is functionally antagonized by UV-DDB2. *J Biol Chem.* (2002) 277:38847–54. doi: 10.1074/jbc.M205722200
77. Martin-Lluesma S, Schaeffer C, Robert EI, Van Breugel PC, Leupin O, Hantz O, et al. Hepatitis B virus X protein affects S phase progression leading to chromosome segregation defects by binding to damaged DNA binding protein 1. *Hepatology* (2008) 48:1467–76. doi: 10.1002/hep.22542
78. Andersen JL, Dehart JL, Zimmerman ES, Ardon O, Kim B, Jacquot G, et al. HIV-1 Vpr-induced apoptosis is cell cycle dependent and requires Bax but not ANT. *PLoS Pathog.* (2006) 2:e127. doi: 10.1371/journal.ppat.0020127
79. Reil H, Hoxter M, Moosmayer D, Pauli G, Hauser H. CD4 expressing human 293 cells as a tool for studies in HIV-1 replication: the efficiency of translational frameshifting is not altered by HIV-1 infection. *Virology* (1994) 205:371–5.
80. Hiscott J, Kwon H, Genin P. Hostile takeovers: viral appropriation of the NF-kappaB pathway. *J Clin Invest.* (2001) 107:143–51. doi: 10.1172/JCI11918
81. Hiebenthal-Millow K, Pohlmann S, Munch J, Kirchhoff F. Differential regulation of human immunodeficiency virus type 2 and simian immunodeficiency virus promoter activity. *Virology* (2004) 324:501–9. doi: 10.1016/j.virol.2004.04.007
82. Chen BK, Feinberg MB, Baltimore D. The kappaB sites in the human immunodeficiency virus type 1 long terminal repeat enhance virus replication yet are not absolutely required for viral growth. *J Virol.* (1997) 71:5495–504.
83. Moriuchi H, Moriuchi M, Fauci AS. Nuclear factor-kappa B potently up-regulates the promoter activity of RANTES, a chemokine that blocks HIV infection. *J Immunol.* (1997) 158:3483–91.
84. Manganaro L, De Castro E, Maestre AM, Olivieri K, Garcia-Sastre A, Fernandez-Sesma A, et al. HIV Vpu interferes with NF-kappaB activity but not with interferon regulatory factor 3. *J Virol.* (2015) 89:9781–90. doi: 10.1128/JVI.01596-15
85. Hotter D, Krabbe T, Reith E, Gawanbacht A, Rahm N, Ayoub A, et al. Primate lentiviruses use at least three alternative strategies to suppress NF-kappaB-mediated immune activation. *PLoS Pathog.* (2017) 13:e1006598. doi: 10.1371/journal.ppat.1006598
86. Akari H, Bour S, Kao S, Adachi A, Strebel K. The human immunodeficiency virus type 1 accessory protein Vpu induces apoptosis by suppressing the nuclear factor kappaB-dependent expression of antiapoptotic factors. *J Exp Med.* (2001) 194:1299–311. doi: 10.1084/jem.194.9.1299
87. Bour S, Perrin C, Akari H, Strebel K. The human immunodeficiency virus type 1 Vpu protein inhibits NF-kappa B activation by interfering with beta TrCP-mediated degradation of Ikappa B. *J Biol Chem.* (2001) 276:15920–8. doi: 10.1074/jbc.M010533200

Conflict of Interest Statement: The authors declare that the research was conducted in the absence of any commercial or financial relationships that could be construed as a potential conflict of interest.

Copyright © 2018 Landsberg, Megger, Hotter, Rückborn, Eilbrecht, Rashidi-Alavijeh, Howe, Heinrichs, Sauter, Sitek, Le-Trilling and Trilling. This is an open-access article distributed under the terms of the Creative Commons Attribution License (CC BY). The use, distribution or reproduction in other forums is permitted, provided the original author(s) and the copyright owner(s) are credited and that the original publication in this journal is cited, in accordance with accepted academic practice. No use, distribution or reproduction is permitted which does not comply with these terms.